

Journal of
**Applied
Crystallography**

ISSN 0021-8898

Editor: **Gernot Kosterz**

A new sample mounting technique for room-temperature macromolecular crystallography

Yevgeniy Kalinin, Jan Kmetko, Adam Bartnik, Andrew Stewart, Richard Gillilan, Emil Lobkovsky and Robert Thorne

Copyright © International Union of Crystallography

Author(s) of this paper may load this reprint on their own web site provided that this cover page is retained. Republication of this article or its storage in electronic databases or the like is not permitted without prior permission in writing from the IUCr.

A new sample mounting technique for room-temperature macromolecular crystallography

Yevgeniy Kalinin,^a Jan Kmetko,^a Adam Bartnik,^{a‡} Andrew Stewart,^b Richard Gillilan,^c Emil Lobkovsky^d and Robert Thorne^{a*}

^aPhysics Department, Cornell University, Ithaca, NY 14853, USA, ^bCornell High-Energy Synchrotron Source, Cornell University, Ithaca, NY 14853, USA, ^cMacromolecular Diffraction Facility, Cornell High-Energy Synchrotron Source, Cornell University, Ithaca, NY 14853, USA, and ^dDepartment of Chemistry and Chemical Biology, Cornell University, Ithaca, NY 14853, USA. Correspondence e-mail: ret6@cornell.edu

A new method for mounting protein crystals and other environmentally sensitive samples for room-temperature diffraction measurements is described. A crystal is retrieved using a microfabricated sample mount as recently reported, and the mount is inserted into a modified goniometer-compatible base. A transparent thin-wall polyester tube sealed at one end and filled with stabilizing liquid is then drawn over the crystal and sealed to the goniometer base. Compared with mounting using glass capillaries, this method can provide lower-background X-ray scattering, especially at higher resolutions; dramatically improved ease of crystal mounting with minimal chance of damage; accurate and reproducible crystal positioning relative to the goniometer base; improved crystal visibility and ease of alignment, especially for very small crystals; and compatibility with high-throughput approaches. Crystals can be rapidly screened and eliminated earlier in the data collection pipeline, and the cause of poor low-temperature diffraction can be diagnosed.

© 2005 International Union of Crystallography
Printed in Great Britain – all rights reserved

1. Introduction

Over the past decade, nearly all macromolecular structures have been determined using cryocrystallographic techniques. Flash-cooling to low temperatures dramatically increases the amount of data that can be collected from a single crystal before radiation damage becomes significant and allows complete data sets to be obtained from very small crystals. Flash-cooling improves crystal stability in other ways, allowing easy storage, transport and data collection in a high-throughput environment.

Despite these major advantages, there are still good reasons to collect data at or near room temperature. Flash-cooling nearly always degrades crystal mosaicity from as-grown values of < 0.01 to 0.1° or more and (unlike for small-molecule crystals) reduces the maximum achievable resolution under optimal data collection conditions. Flash-cooling sometimes causes important changes in molecular structure, so when radiation damage is not significant room-temperature structures may be more accurate. Room-temperature data collection is essential for time-resolved studies of the mechanism and dynamics of protein function, and for the many macromolecular and virus crystals, especially those with large unit cells or large solvent contents, that diffract poorly after flash-cooling. Most importantly to current efforts, room-tempera-

ture data collection can eliminate poorly ordered crystals before serious effort is expended cryoprotecting and flash-cooling them, and can allow the cause of poor low-temperature diffraction (as-grown disorder, disorder induced by post-growth treatment like drug binding and cryoprotectant soaks, or the flash-cooling process itself) to be diagnosed.

One major reason why so few diffraction data are now collected at room temperature is that the required methods are extremely inconvenient. In the most widely used method (Bernal & Crowfoot, 1934), a thin-wall glass capillary is inserted into a crystal-containing drop, and the crystal plus some of the drop solution is sucked up into the capillary by a combination of capillary forces and applied suction. The crystal and liquid are carefully separated, either by wicking the liquid or by using pressure jumps to move the liquid relative to the crystal. To prevent crystal slippage during data collection, excess liquid between crystal and capillary is wicked away. Additional liquid from the drop is added to the capillary to maintain a humid environment. The capillary is then cut to the desired length by crushing, by scribing and breaking, or using a hot wire (for ordinary glass), and sealed at both ends using wax or grease.

Standard $10\ \mu\text{m}$ wall capillaries are extremely fragile and are easily broken during cutting, sealing and routine handling. Drawing crystals up past the hard sharp edges of the capillary's tip is extremely difficult to control and frequently damages them, especially when the crystals have rod- or plate-

‡ Present address: School of Applied and Engineering Physics, Cornell University, Ithaca, NY 14853, USA.

like morphologies. Accurate and reproducible positioning of crystals within the capillary requires great skill. Residual liquid holding the crystal against the curved capillary wall creates substantial optical distortion, making accurate optical alignment of smaller crystals very difficult. Capillary forces

exerted by this liquid can bend and broaden the mosaicity of rod- or plate-like crystals. X-ray absorption by the capillary during data set collection depends on the crystal's orientation within it, and is non-reproducible and unpredictable (Teng, 1990). Once data collection is complete, the crystal is almost impossible to retrieve without causing (additional) damage, so that comparison of room- and low-temperature data from the same crystal is impractical. Capillary fragility also makes changing the liquid inside the capillary for *in situ* ligand soaks or dehydration challenging.

To overcome these problems, many groups have mounted crystals on a support (a glass fiber or a nylon loop) and then enclosed the crystal and support in a large-diameter glass capillary or in the flared end of a capillary [for recent examples, see Mac Sweeney & Arcy (2003) and Basavappa *et al.* (2003)]. Crystals can then be more easily inserted into the capillaries and removed for subsequent flash-cooling. However, the large amount of liquid that holds a crystal in the loop allows crystal movement during data collection, increases background scatter, and makes optical alignment difficult. The loops bend and move, and so crystal positioning with respect to both the goniometer base and the capillary is not reproducible.

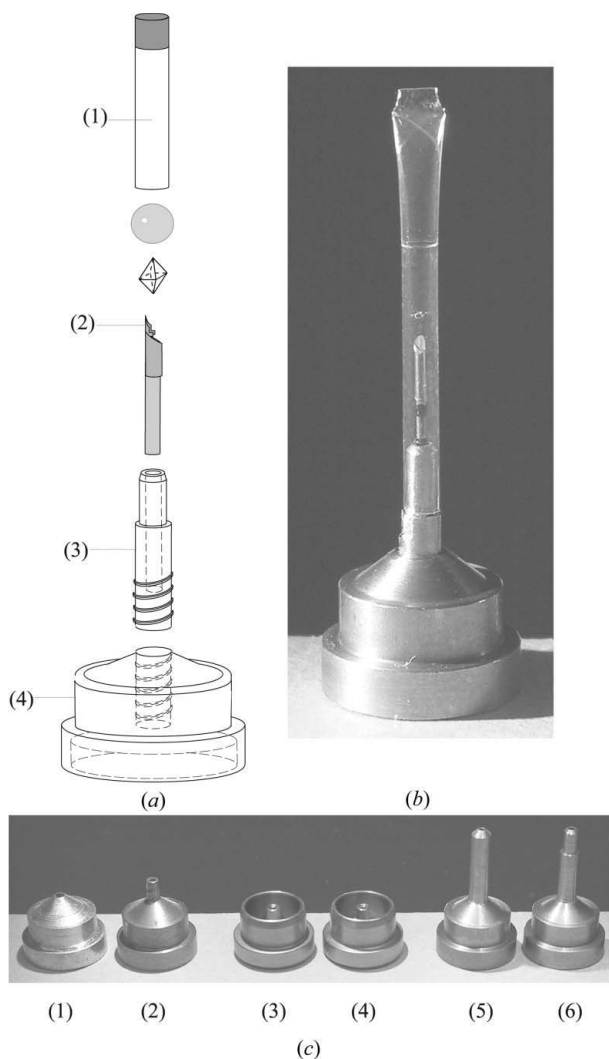


Figure 1 (a) Schematic diagram of a room-temperature mounting technology consisting of (1) a thin-wall polyethylene terephthalate (PET) tube, (2) a microfabricated crystal holder attached to a stainless-steel rod, and a goniometer base composed of (3) a copper post adapted to capture and seal with the tubing and (4) a threaded magnetic stainless-steel base. The tubing is sealed at one end using grease or wax or by thermal impulse compression, and a volume of liquid is injected into the tubing as close to the sealed end as possible. (b) Photograph of the room-temperature mount in (a). (c) Standard goniometer-compatible bases used in cryocrystallography can be easily modified to capture the PET tubing and allow data collection at both room and low temperature. (1) is the most common base style, modified in (2) by addition of a post with a bevelled tip, whose diameter matches the inside diameter of the PET tubing. (3) shows the SPINE base, modified in (4) by reducing the diameter of its central post to match the PET tubing. (5) shows a base sometimes used to reduce frost accumulation during data collection, consisting of a copper post threaded into a stainless-steel base; in (6) it is modified by reducing the copper post's outer diameter near the sample to match the PET tubing.

2. Crystal mount design and mounting protocol

Fig. 1(a) shows the design of our room-temperature mounts. They consist of (1) a short piece of thin-wall (12.5–50 μm) optically transparent poly(ethylene terephthalate) (PET) tubing with a fixed crystal-size-independent diameter of roughly 2 mm; (2) a microfabricated polyimide mount precisely attached to a solid stainless-steel rod, as described previously (Thorne *et al.*, 2003); and (3,4) a magnetic stainless-steel goniometer-compatible base that captures the rod and seals with the PET tubing.

To prepare a sample for X-ray data collection, the stainless-steel rod attached to the polyimide mount (2) is inserted into the goniometer-compatible base (3,4), and held in place using glue or grease. A piece of PET tubing is sealed at one end, using either grease, epoxy or (our preferred method) a thermal impulse compression sealer. A plug of stabilizing solution (used to maintain a humid environment during storage and data collection) is injected using a syringe needle as close to the sealed end of the tubing as possible. Next, a crystal is retrieved from a drop of solution using the polyimide mount (2) and excess liquid is removed [as discussed by Thorne *et al.* (2003)]. Finally, the PET tubing (whose inside diameter of 2 mm is roughly three times the outer dimensions of the mount and rod) is pushed over the mount and onto the base (3,4), with which it forms an airtight seal. A small amount of oil or grease applied to the base can be used to ensure the integrity of the seal. Fig. 1(b) shows a photograph of the completed assembly. Fig. 1(c) shows possible designs of the goniometer-compatible base, to be described in greater detail in §3.3.

3. Detailed description of mount components

3.1. Polyester tubing

The tubing is manufactured by Advanced Polymers Inc. from poly(ethylene terephthalate), a hard, stiff, strong polyester that absorbs little water, has excellent gas barrier properties compared with other polymers and is used in soda bottles. In contrast with glass and quartz capillaries, thin-wall PET tubing is extremely robust. It cannot be broken or torn and resists permanent deformation when squeezed or bent. It can be easily cut to a desired length using scissors or razor blades, with 'extra keen' blades providing the cleanest cuts. It can be thermally sealed using standard impulse compression sealers and is also heat-shrinkable at relatively low temperatures of 473 K. These features make it ideal both for manual use and for use by automated handling equipment in a high-throughput environment. In particular, impulse compression sealing produces a flat squared-off end that can easily be recognized and grabbed by a robotic manipulator. At the

other end, spot impulse heating can be used to shrink-seal the tubing to the post.

PET tubing has superior diffraction properties. Glasses have higher densities ($\sim 2.6 \text{ g cm}^{-3}$ versus $1.3\text{--}1.4 \text{ g cm}^{-3}$ for PET) and contain high atomic number elements (Si and O in quartz glass, with additional B, K, Na and Al in borosilicate glass) versus C, H and O in polyesters. Consequently, for a given wall thickness, glass tubing produces stronger diffuse scattering than PET tubing. PET, being processed at much lower temperatures than glass and being derived from oil instead of rock, also has much smaller concentrations of metallic impurities. We focus here on a comparison with quartz glass, which has a linear absorption coefficient that is much lower than that of soda or special glass and 5–10% larger than that for borosilicate glass (Hilgenberg, 2004).

Fig. 2 compares the diffuse X-ray diffraction patterns at $\lambda = 0.92 \text{ \AA}$ (13.5 keV) produced by (a) a $10 \mu\text{m}$ wall quartz glass capillary with (b) 50, (c) 25 and (d) $12.5 \mu\text{m}$ wall PET tubing, recorded on CHESS beamline F1. Similar data were obtained

on a laboratory diffractometer using the Mo $K\alpha$ edge. In all cases the PET tubing produces less diffuse scatter than the quartz capillary. Fig. 3(a) compares the integrated diffuse intensity of these four samples. The $12.5 \mu\text{m}$ PET produces 80% less diffuse scatter than $10 \mu\text{m}$ quartz glass but for conveniently large diameters is prone to permanent deformation when kinked. The $25 \mu\text{m}$ tubing, which for a diameter of 2 mm has excellent mechanical properties, excellent transparency and is suitable for routine use, produces 60% less diffuse scatter. This improvement should be roughly wavelength independent away from elemental absorption edges (Hubbell & Seltzer, 1996; Berger *et al.*, 1999) and should be particularly useful for small, weakly diffracting crystals. To take full advantage of this reduction, diffuse scatter from air in the path from sample to detector should be minimized by, for example, replacing air with helium.

As seen in Fig. 2, PET's scattering is not isotropic, reflecting the partial longitudinal alignment of the drawn polymer. Fig. 3(b) compares the diffuse intensity for PET and quartz glass, measured along a horizontal line in Fig. 2 passing through the maxima of PET's scattering and the direct beam position. The maximum diffuse scattering for PET occurs at a

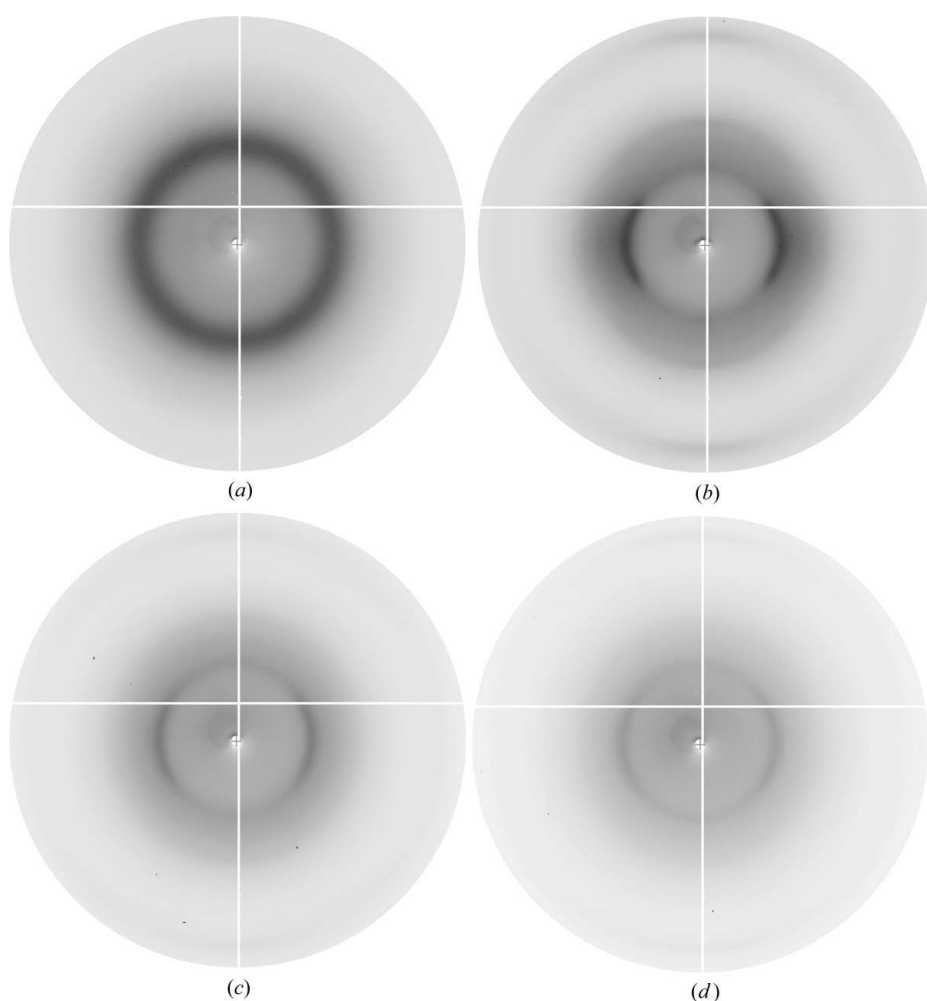


Figure 2 X-ray diffraction images to a maximum resolution of 1.77 \AA recorded at CHESS ($\lambda = 0.92 \text{ \AA}$) from (a) a quartz capillary with $10 \mu\text{m}$ thick walls, (b) PET tubing with $50 \mu\text{m}$ thick walls, (c) PET tubing with $25 \mu\text{m}$ thick walls and (d) PET tubing with $12.5 \mu\text{m}$ thick walls. Intensity scales are the same for all images, and contributions to background scatter from air have not been subtracted.

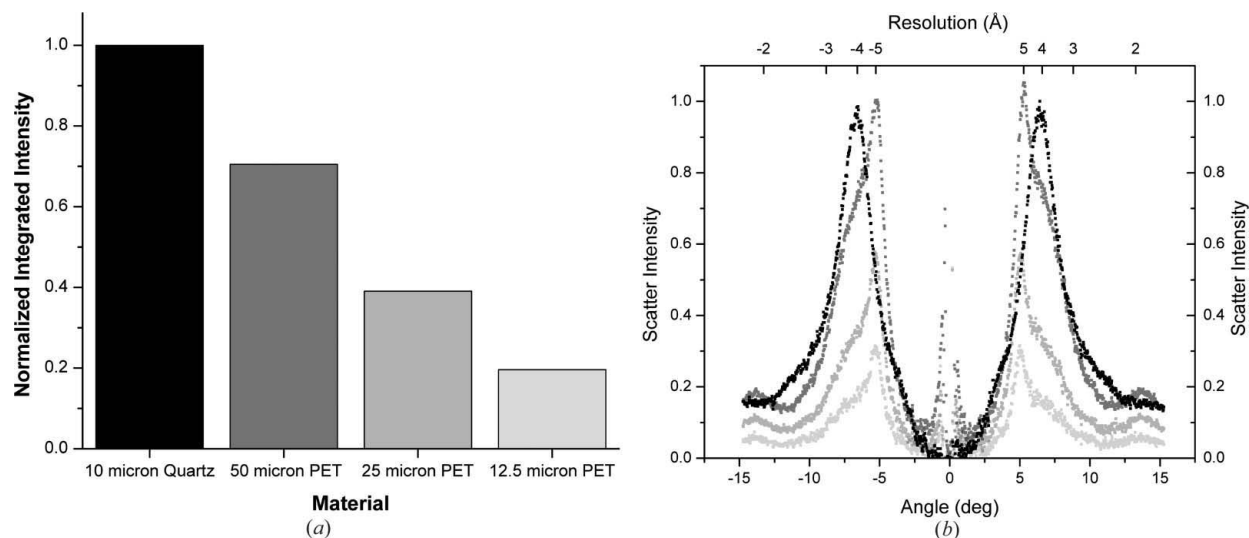


Figure 3 (a) Comparison of integrated diffuse X-ray diffraction intensities obtained from Fig. 2 for quartz glass and PET tubing of different thicknesses, out to the full frame resolution of 0.95 Å. The background contribution due to air scattering has been subtracted out. (b) Normalized diffraction intensity *versus* angle and resolution along a horizontal line passing through the direct beam position from Fig. 2, for quartz glass and PET tubing. Along a vertical line, the maximum for the 25 µm PET tubing is reduced relative to the maximum along the horizontal line by a factor of 1.6. The greyscale assignments are the same in (a) and (b).

smaller angle/lower resolution than for most glasses. Consequently, PET provides an even larger improvement in diffraction-signal-to-diffuse-background ratio in the important 4.4–2.2 Å resolution region than Fig. 3(a) suggests.

The only disadvantage of thin-wall PET is that, unlike glass, it is somewhat permeable so that vapor will diffuse in or out of the tubing. With time, this diffusion will change the solute concentrations in the liquid plug and may dehydrate the crystal. However, our measurements suggest that permeability and dehydration will not be important in most applications. To evaluate this permeability, pure water (25 µl) was injected into 2 mm diameter, 38 mm long pieces of PET tubing, producing a water plug approximately 8 mm long. The ends of the tubing were sealed using either vacuum grease or thermal impulse compression. To characterize the effects of temperature, tubing samples were left in ambient laboratory conditions and placed uncovered in a refrigerator. To vary the relative humidity (r.h.) of the surrounding environment, the tubing was sealed in 50 ml jars which contained ~10 ml of saturated solutions of various salts (Rockland, 1960; Dobrianov *et al.*, 2001) giving room-temperature r.h. values of 11, 23, 33, 57, 75 and 86%. The weight of tubing + liquid was measured at regular intervals over a period of several days.

Fig. 4 shows evaporation rates of pure water for 12.5, 25 and 50 µm tubing measured at 295 (2) K in a room with ordinary air circulation and an ambient relative humidity of 50 (5)% (light grey bars), and at 277 (2) K in a refrigerator with moderate air circulation and a relative humidity of 40 (5)% (dark grey bars). For our preferred 25 µm wall thickness, the mass change rate was roughly 1.8 mg d⁻¹ at 295 K and 50% r.h., and 0.6 mg d⁻¹ at 277 K and 40% r.h. At 295 K, the measured mass change rate variation with relative humidity of the environment is fit by a straight line with a slope of -0.013 mg d⁻¹ (% r.h.)⁻¹ and an intercept at 0% r.h. of

2.2 mg d⁻¹, varying between 2.2 and 1 mg d⁻¹ for r.h. between 11 and 100%. Measurements *versus* total tubing length at 295 K and 50% r.h. give a rate of roughly 0.6 mg d⁻¹ per centimeter of length. We have also studied 2 mm diameter, 25 µm wall polyimide tubing manufactured by MicroLumen. Polyimide gave an evaporation rate 50% larger than that of PET tubing and had inferior optical properties and so was not studied further.

Diffusion through the tubing wall will change the concentration of solutes in the liquid plug and dehydrate/dissolve the crystal. However, for 25 µm wall tubing and liquid volumes

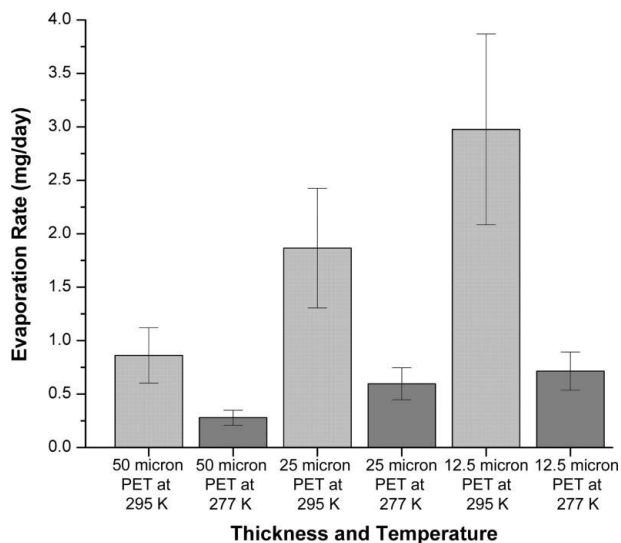


Figure 4 Average evaporation rates in milligrams per 24 h interval from 38 mm of PET tubing with wall thicknesses of 12.5, 25 and 50 µm, measured at 295 (2) K and 50 (5)% relative humidity (light grey bars) and 277 (2) K and 40 (5)% relative humidity (dark grey bars). The tubing was initially filled with 25 µl of pure water.

comparable to that used in Fig. 4, this concentration change will be small ($\sim 5\%$) during a typical 18 h data collection time on a low-power laboratory X-ray source; negligible ($< 0.3\%$) during data collection at a synchrotron source; and irrelevant when screening crystals at room temperature before flash-cooling. Fig. 5 shows X-ray data from a tetragonal lysozyme crystal (*a*) mounted in a quartz capillary and (*b*) after remounting using the present method in 25 μm wall PET tubing and 18 h of storage at ambient conditions. The diffraction resolution, mosaicity and unit-cell parameters remain the same.

The fractional vapor exchange rate through the tubing can be reduced in several ways. The tubing thickness can be increased, at the expense of optical clarity and background diffracted intensity, and its length can be decreased. The effective tubing length for vapor exchange can be reduced while preserving its X-ray properties and liquid-holding

capacity by coating the tubing beyond the crystal with vacuum grease, dipping it into a fast-drying polymer solution, or depositing a thin film of metal or other vapor barrier material (a service provided by several companies.) Vapor exchange can be reduced by increasing the volume of the liquid plug, by increasing the plug length and/or by increasing the tubing diameter. In practice, a gap of 2–4 mm should be maintained between the plug and crystal to minimize the chance of crystal contact with liquid caused by air/liquid interface motions during handling. Increasing the liquid plug length L_p by ΔL_p (and thus the overall tubing length L to $L + \Delta L_p$) increases the liquid-volume-to-tubing-surface-area ratio by a factor $1 + \Delta L_p/L_p$ (for $L_p, \Delta L_p \ll L$) and should thus increase the time required to reach a given fractional solvent loss and dehydration. Similarly, increasing the tubing diameter from d to $d + \Delta d$ (for fixed L_p) increases the liquid-volume-to-tubing-surface-area ratio by $1 + \Delta d/d$ (for $\Delta d \ll d$). Larger tubing diameters have the added advantage of providing more clearance when the tubing is drawn over the crystal. However, increasing the tubing diameter reduces the ratio of the capillary forces that hold the liquid in place to the drop's mass by a factor $1 - \Delta d/d$ ($\Delta d \ll d$) and thus makes plug movement during the accelerations associated with handling more likely. We find that a tubing diameter of 2 mm with a wall thickness of 25 μm provides a good compromise between ease of handling, mechanical stability, liquid plug stability, dehydration rate, crystal visibility and X-ray diffuse scattering. Liquid plug stability can be enhanced by injecting the liquid down into the sealed end of the tubing and leaving no air gap between the liquid plug and seal.

Glass capillaries with epoxy, grease or (much less reliably) wax seals can allow crystals to be stored for months. When using PET tubing for data collection, long-term storage can be achieved by keeping the sample in a glass bottle having a reservoir solution that maintains equilibrium with the crystal and liquid plug. This reservoir liquid can be contained using a sealed, semipermeable PET tube or a plastic bag. Alternatively, the PET tubing can be removed and replaced with glass or thick wall plastic tubing with the same inner diameter. However, we expect long-term storage to be less of an issue than when using glass capillaries; mounting crystals for room-temperature experiments using the present method is trivial and can be performed with high confidence of success immediately before data collection.

3.2. Microfabricated crystal mount

In recent attempts to simplify the capillary mounting method (*e.g.* Mac Sweeney & Arcy, 2003; Basavappa *et al.*, 2003), the crystal was mounted in a standard flexible nylon loop used for cryocrystallography. Then either the crystal was deposited onto a capillary wall using the loop, or a glass capillary was drawn over the loop and sealed to a putty-filled base. We recently described a new technology for mounting crystals for cryocrystallography that improves on nylon loops in every important way (Thorne *et al.*, 2003). The loop is replaced by a thin microfabricated polyimide film that is

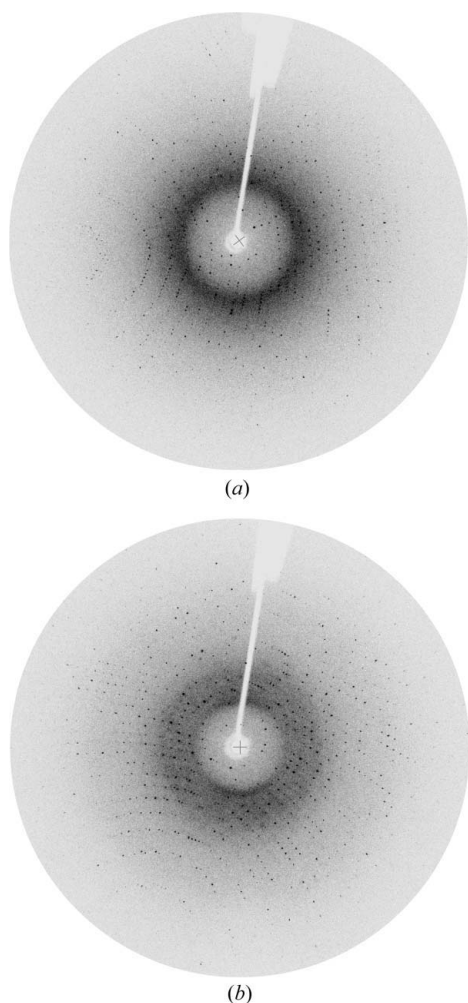


Figure 5

(*a*) X-ray diffraction pattern recorded from a 400 μm lysozyme crystal mounted in a 10 μm wall quartz glass capillary using standard procedures. The crystal diffracts to about 1.65 \AA . (*b*) X-ray diffraction pattern recorded from the same crystal, acquired 18 h after removal from the quartz capillary and remounting in 25 μm wall PET tubing using the procedure described here. The diffraction resolution, mosaicity and unit-cell parameters are unchanged.

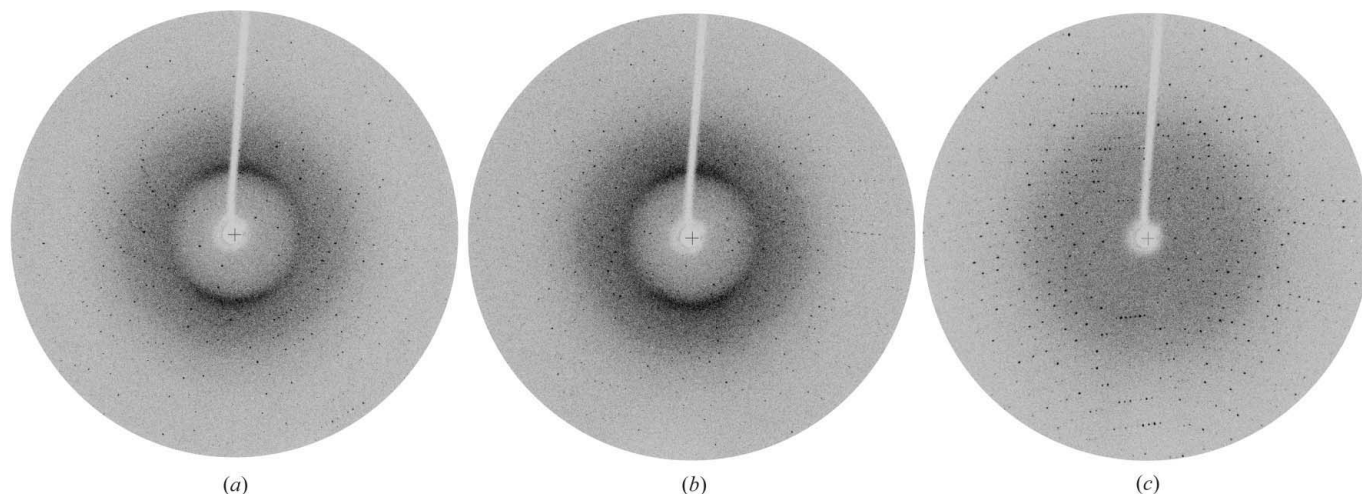


Figure 6
X-ray diffraction patterns acquired from (a) a 120 μm lysozyme crystal mounted in 25 μm thick PET tubing, (b) the same crystal remounted in PET tubing after a cryoprotection soak and (c) the same crystal (with PET tubing removed) after flash-cooling. The diffraction resolution remains unchanged while the mosaicity of the frozen crystal has increased.

curved by wrapping around a stainless-steel rod to give the film rigidity. The film has an aperture for the crystal connected *via* a channel to a larger aperture, into which a wick can be inserted to remove excess surrounding liquid. This technology reduces background X-ray scatter; simplifies manipulating and mounting crystals, especially in the 5–200 μm size range; eliminates crystal/mount bending and vibrations; and simplifies manual and automated alignment. In the present application, this method has three overwhelming advantages. Firstly, since the polyimide mount is rigid, the crystal's lateral and vertical position with respect to the stainless-steel rod are completely reproducible and the crystal is always held close to the rod axis. In contrast, the flexibility and natural twist of nylon loops often leave the crystal far outside the rod's outer diameter. Consequently, with microfabricated mounts the PET tubing (or, if desired, glass capillary) can be easily drawn over the crystal and rod with minimal risk of bumping the crystal, which is important for both manual and automated assembly. Secondly, the microfabricated mount's aperture can be selected to match the crystal size so that the crystal is 'glued' to the mount by the capillary forces of a very small amount of liquid. In contrast, loops have poorly defined size and shape, and crystals (particularly those smaller than 100 μm) are usually suspended in a large volume of liquid spanning the loop aperture. Consequently, microfabricated mounts reduce the chance of crystal slippage and diffraction pattern shifts as the crystal is rotated during data collection, and reduce background scatter from excess liquid. Thirdly, the microfabricated mount contains alignment marks and a crystal aperture size code that allow automated alignment and beam size selection without optical observation of the crystal itself.

3.3. Goniometer-compatible bases

Fig. 1(c) shows how existing goniometer-compatible magnetic stainless-steel bases used in cryocrystallography can

be modified to capture the PET tubing, allowing room- and low-temperature data to be collected from the same crystal without dismounting it. In (2), a small tapered cylindrical extension is added to the most common base style (1). In (4), the outside diameter of the central post of the SPINE base (3) (Spine Structural Genomics in Europe, 2002) is slightly reduced to match the tubing's inside diameter.

Base (6), derived from base design (5), sometimes used to reduce icing, has particular advantages. A threaded copper post is screwed into a magnetic stainless-steel base. The post has a rod-capturing hole and a reduced diameter tip to capture the tubing. Extending the length of this post to within a few millimeters of the crystal position minimizes the length of tubing that must be drawn past the crystal to make a seal, thus making assembly much easier. This also reduces liquid loss rates by reducing the length of tubing below the crystal through which diffusion can occur.

4. Mount evaluation and performance

The technology described here has several advantages over mounting in glass capillaries. Crystal mounting and removal is much easier and faster, with little risk of crystal damage, and background X-ray scatter from the tubing is much smaller. Crystals can be rapidly screened for diffraction quality at room temperature before time is invested cryoprotecting and flash-cooling them, allowing a large increase in throughput. Collecting room- and low-temperature data from the same crystal is straightforward, so that a few room-temperature frames can set a benchmark for achievable low-temperature resolution and mosaicity and/or can diagnose the cause of poor low-temperature diffraction. This is demonstrated in Fig. 6, which shows X-ray diffraction data collected from the same lysozyme crystal (a) at room temperature (in PET tubing), (b) at room temperature (in PET tubing) after it was soaked using

the microfabricated mount in a cryoprotective solution, and (c) after flash-cooling (with the PET tubing removed).

Unlike in glass capillary mounting, crystals having a wide range of sizes can be mounted using only a single diameter of PET tubing, and a single piece of PET tubing can be reused for multiple crystals, reducing the cost per measurement.

Aligning the crystal in the X-ray beam is greatly simplified. In capillary mounting, the capillary wall together with the liquid that holds the crystal against it form a highly distorting lens, making alignment of small crystals especially difficult. The present technology places the crystal in the middle of the tubing with minimal surrounding liquid. Fig. 7 shows that there is some residual distortion caused by circumferential variations of the wall thickness of the extruded PET tubing. For 2 mm diameter, 25 μm wall PET tubing the maximum image displacement normal to the tubing axis is roughly 30 μm , and the displacement along the axis is an order of magnitude smaller. With these uncertainties both automated and manual alignment should still be straightforward, although some orientation averaging may be required for very small (< 50 μm) crystals.

Residual liquid around the crystal is reduced compared with conventional capillary mounting and with capillary mounting using nylon loops (Mac Sweeney & Arcy, 2003; Basavappa *et al.*, 2003). Therefore, background X-ray scatter (important for small crystals) and crystal slippage during rotations (important for larger crystals) are also reduced. However, if the liquid volume holding the crystal to the microfabricated mount is too small, percussive forces can knock the crystal off the mount. To ship mounted samples, excess liquid can be left around the crystal and then removed prior to data collection. Alternatively, samples can be mounted at the beamline or can be shipped frozen after room-temperature checks on a laboratory source.

5. Conclusions

We have described a simple inexpensive technology that makes mounting and collecting diffraction data from crystals at room temperature as easy as at low temperatures, and that allows room- and low-temperature data to be collected from the same crystal. This technology will allow the benefits of room-temperature data collection, especially in rapid and efficient elimination of poorly ordered crystals and in the diagnosis of poor low-temperature diffraction, to be conveniently exploited in both traditional and high-throughput environments. The superior properties of polyester tubing demonstrated here also make it an attractive candidate for use in capillary-based high-throughput crystallization.

The authors thank Craig Downie, Angela Toms and the members of Professor Steven Ealick's group for their assistance in X-ray data collection and analysis. This work was

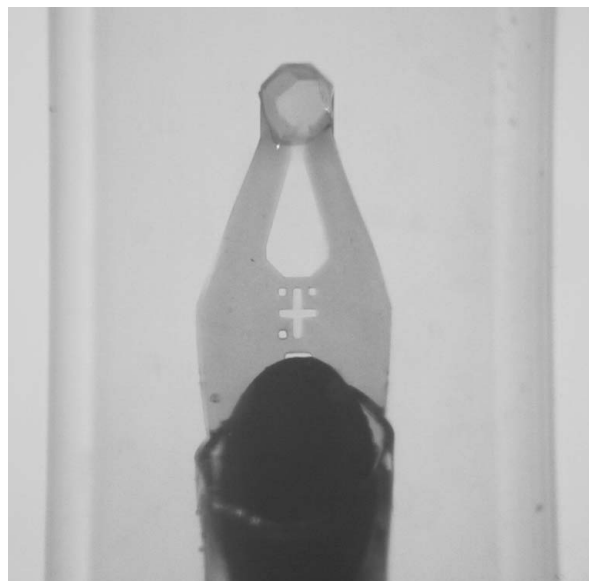


Figure 7

A crystal held on a microfabricated polyimide mount inside PET tubing. Some optical distortion is evident due to circumferential tubing thickness variations created by the tubing extrusion process.

supported by the NIH (R01 GM65981-01) and by NASA (NAG8-1831). Microfabrication was performed at the Cornell Nano-Scale Science and Technology Facility (a member of the National Nanofabrication Users' Network) which is supported by the National Science Foundation under grant ECS-9731293, its users, Cornell University and Industrial Affiliates. CHESS and MacCHESS are, respectively, supported by the National Science Foundation (DMR 97-13424) and by the NIH through its National Center for Research Resources (RR-01646).

References

- Basavappa, R., Petri, E. T. & Tolbert, B. S. (2003). *J. Appl. Cryst.* **36**, 1297–1298.
- Berger, M. J., Hubbell, J. H., Seltzer, S. M., Coursey, J. S. & Zucker, D. S. (1999). *XCOM: Photon Cross Sections Database*. <http://physics.nist.gov/PhysRefData/Xcom/Text/XCOM.html>.
- Bernal, J. D. & Crowfoot, D. (1934). *Nature (London)*, **133**, 794–795.
- Dobrianov, I., Kriminski, S., Caylor, C. L., Lemay, S. G., Kisselev, A., Finkelstein, K. D. & Thorne, R. E. (2001). *Acta Cryst.* **D57**, 61–68.
- Hilgenberg (2004). <http://www.hilgenberg-gmbh.de/index.php?id=markroehrchen0andL=1>.
- Hubbell, J. H. & Seltzer, S. M. (1996). *Tables of X-ray Mass Attenuation Coefficients and Mass Energy-Absorption Coefficients*. <http://physics.nist.gov/PhysRefData/XrayMassCoef/cover.html>.
- Mac Sweeney, A. & D'Arcy, A. (2003). *J. Appl. Cryst.* **36**, 165–166.
- Rockland, L. B. (1960). *Anal. Chem.* **32**, 1375–1376.
- Spine Structural Genomics in Europe (2002). *Spine Sample Holder and Vial Specifications*. http://www.spineurope.org/page.php?page=protocol_vials.
- Teng, T. Y. (1990). *J. Appl. Cryst.* **23**, 387–391.
- Thorne, R. E., Stum, Z., Kmetko, J., O'Neill, K. & Gillilan, R. (2003). *J. Appl. Cryst.* **36**, 1455–1460.